Electron spin resonance studies in the doped polyaniline PANI-AMPSA: Evidence for local ordering from linewidth features

V. Sitaram,[1] Ajay Sharma,[1] S. V. Bhat,[1] K. Mizoguchi,[2] and Reghu Menon[1]
[1]*Department of Physics, Indian Institute of Science, Bangalore-560 012, India*
[2]*Department of Physics, Tokyo Metropolitan University, Hachi-oji, Tokyo, Japan*

X-band electron spin resonance (ESR) of polyaniline (PANI) doped with 2-acrylamido-2-methyl-1-propane sulfonic acid (AMPSA), at conductivity values of 90, 4, and 0.2 S/cm, has been investigated from 300 to 5 K. Free-standing films (30–40 μm thick) of PANI were prepared by solution casting method. The spectra consist of two signals, one is broad ($\sim$60 G) and the other is narrow ($\sim$10 G), at nearly the same resonance field. The temperature variation of ESR susceptibility indicates a stronger Pauli component in the broad line signal, as compared to the narrow signal, at all values of conductivity. Both linewidths are independent of the presence of O_2. The temperature variation of linewidths is explained in terms of the quasi-two-dimensional (Q2D) model. These results suggest that in some regions the doped PANI chains have self-assembled Q2D structure, and the presence of a significant Pauli susceptibility indicates that the charge carriers are highly delocalized in these Q2D regions.

I. INTRODUCTION

The electronic states of conducting polymers have attracted a great deal of attention and have been investigated in detail.[1] ESR of doped conjugated polymers reveals information about the electronic states, spin and charge dynamics; it is also an independent measure of properties such as susceptibility and transport.[1–4] The previous studies of spin dynamics have enabled the probing of conduction process at the microscopic scale, and to understand the nature of the limiting processes in nanoscopic scale conductivity.[5–7] Various conducting polymers have been studied to understand the underlying mechanisms of spin and charge transport. Polyaniline (PANI) is an important material due to its ease of preparation and stability. PANI is unique in the fact that its doping process is not the typical redox reaction, and the number of electrons in the chain remains constant.[8] This doping via protonation leads to a lattice distortion (quinoid-benzoid) with hole carriers on PANI chain. PANI can be easily processed in both insulating (emeraldine base) and conducting (emeraldine salt) forms. The recent advances in the synthesis, doping and processing of PANI using surfactant counterions, have improved the morphology and conductivity. Doping of PANI with various dopants like dodecyl benzoyl sulfonic acid (DBSA), camphor sulfonic acid (CSA) and other sulfonic acids has lead to much better quality samples.[9–11]

The improvement in processing of doped PANI films by surfactant counterions has assisted the long-range ordering of PANI chains, and this has enhanced the metallic nature. However, the mechanism of charge transport and spin dynamics, as a function of sample morphology, are yet to be understood in detail. For example, the extended and coiled structure of chains can give raise to wide range of nanoscopic scale morphological features, and this in turn determines the relative number of polarons, bipolarons and free carriers in the system, and the associated charge and spin dynamics. In previous generation of doped PANI, the formation of bipolarons (charge $2e$ and spin 0) was proposed to account for depletion of spins at higher doping levels.[12–14] In those samples, a large Curie susceptibility and a small Pauli contribution, especially at high temperatures, were observed. This was explained by spinless bipolaron model, where the Curie susceptibility was attributed to defects in the sample.[14] In the new surfactant counterion processed samples, a large Pauli contribution has been observed for a wide range of temperatures ($T > 50$ K), with a weak Curie term, as a function of increasing doping levels.[15] In this system, Sariciftci *et al.* have observed that a Fermi glass model is appropriate to explain the temperature dependence of magnetic susceptibility.[15]

In this paper we present the ESR study, along with SQUID data, of PANI doped with 2-acrylamido-2-methyl-1-propane sulfonic acid (AMPSA), from 300 to 4 K. This sample has a room temperature conductivity of 90 S/cm (fully doped), and the conductivity at 1.6 K is nearly 37 S/cm. Although this conductivity of 90 S/cm is barely on the metallic side of metal-insulator (MI) transition for PANI-AMPSA, the positive temperature coefficient of resistivity persists down to 100 K, indicating intrinsic metallic features. The metallic nature has also been confirmed by magnetoresistance measurements.[16,17] We correlate these transport results with the ESR data in this work. The ESR experiments were performed both in presence of oxygen (ambient air) and in vacuum. The dedoped samples [$\sigma \sim 4$ and 0.2 S/cm], in which the original sample morphology is nearly retained, were studied to understand the system at lower doping levels.

The ESR results of PANI-AMPSA indicate certain interesting features. The presence of a double line feature (one broad and another narrow) has clearly been observed in case of PANI-AMPSA. The intensity of both lines is dependent on doping level. However, the linewidth is nearly independent of oxygen presence. These special features in PANI-

AMPSA are analyzed by taking into account of a special dopant-polymer chain interaction in this system. We propose that these interactions result in a self-assembled quasi-two-dimensional (Q2D) structure. This leads to interesting differences in spin-relaxation (and transport properties), as compared to other doped PANI systems. These results indicate that it is possible to develop self-organized structures in conducting polymers by choosing the appropriate combination of polymer-dopant interactions.

II. EXPERIMENT

Polyaniline was synthesized at −40 °C.[18] Appropriate amounts of PANI and AMPSA powders were mixed in mortar and pestle. The powders were then added to dichloroacetic acid (DCA) and stirred under nitrogen atmosphere at 200 000 rpm for ~10 min. The solution thus obtained was centrifuged and cast onto glass substrates and dried at 60 °C. After drying, the films (thickness: 60–30 μm) were peeled off from the substrate.

The ESR measurements were carried out at 9.42 GHz (X band) with a Bruker spectrometer (model 200 D), equipped with an Oxford Instruments continuous-flow helium cryostat (down to 5 K, model ESR 900) with a temperature accuracy of ±1 K. The oxygen dependence of linewidth was verified *in situ* by connecting the ESR sample tube to a vacuum system and measuring the linewidth at various levels of vacuum down to 10^{-3} torr. The linewidth showed hardly any change even upon repeated evacuation and readmission of air. The efficiency of the evacuation process was checked by repeating the same procedure with metallic polypyrrole PPy-PF_6 samples ($\sigma \sim 300$ S/cm). The measurements in PPy-PF_6 sample follow the reported values: ~2 G in air and 0.2 G in vacuum.[19,20] For the data shown in present work, the PANI-AMPSA sample was evacuated for 6 hours at 10^{-5} torr in an ESR silent standard quartz tube and sealed with small amount of helium gas, for thermal contact at low temperatures. The absence of any oxygen-moisture dependence in the linewidth for PANI-AMPSA is indeed surprising, with respect to other conducting polymers.[21] The linewidths for broad and narrow lines in PANI-AMPSA are approximately 60 and 12 G, respectively. In several samples these values are consistently observed. These linewidths are considerably larger with respect to that usually observed in other doped conducting polymers [for, e.g., PANI-CSA ~0.2 G, PPy-PF_6 ~0.2 G]. Moreover, the ESR spectra of undoped PANI and AMPSA were also recorded separately; also in the physically mixed together sample of PANI with AMPSA at various proportions. While pure PANI and AMPSA give negligible ESR signals at maximum gain of equipment, PANI+AMPSA powder mixture shows linewidths of around 2 G in air. Electrochemically synthesized films of PPy-AMPSA ($\sigma \sim 10$ S/cm) shows a linewidth of 4.5 G in air, with a weak oxygen dependence of the linewidth. These controlled experiments confirm that the large linewidth is intrinsic to the solution-casted film of PANI-AMPSA in DCA.

The fully doped PANI-AMPSA samples were dedoped (deprotonated) to lower values of conductivity by exposing them to ammonia vapor in a well-controlled manner. The same sample was successively dedoped to ensure that the same morphology is retained as the conductivity is lowered down to 0.2 S/cm. A low concentration of ammonia solution and long duration of exposure to its vapors (~10 days) is used to ensure that the deprotonation process is fairly uniform. The *in situ* measurement of conductivity showed no jumps during dedoping process, and the samples were allowed to stabilize before ESR experiments were performed. The dedoping by means of ammonia is not expected to alter the ordering of PANI chains significantly. This allows us to independently control and study the effects of fixed spin scattering and mobility induced variations in the linewidths, without the role of sample-to-sample morphology induced changes in the linewidth.

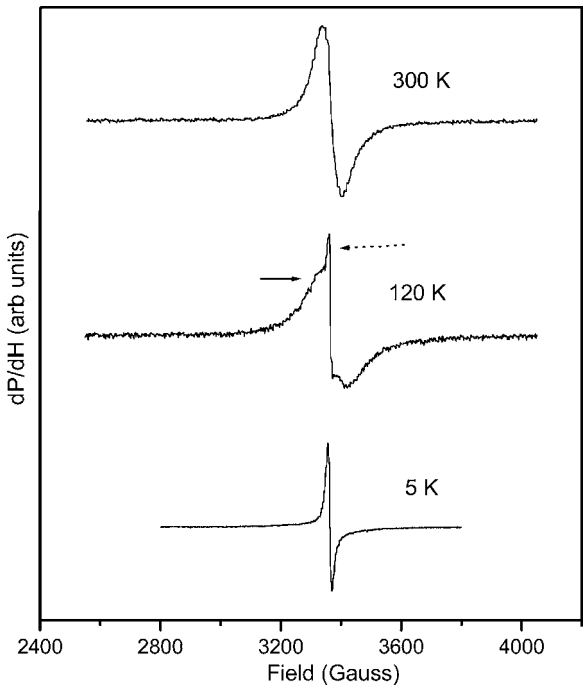

FIG. 1. X-band (9.42 GHz) ESR data (raw) of PANI-AMPSA, for fully doped sample (σ=90 S/cm) at temperatures 5, 120, and 300 K. The markers at 120 K show the presence of two lines.

III. RESULTS AND DISCUSSION

Two ESR signals (one broad and one narrow) were recorded at all temperatures and doping levels. The raw data is shown in Fig. 1. The lines fitted to Eq. (1), are shown in Fig. 2. This shows the coexistence of two weakly asymmetric lines at nearly the same H_0 value, with the narrower line generally downshifted by about 3 G in the field. The evolution of the double line feature is clear at intermediate temperatures ($T < 250$ K); and the narrow line is observed to predominate at lower temperatures. Both the lines fit well with a weak Dysonian, and the spectrum is given by

$$\chi = \chi_{abs} \cos\phi + \chi_{disp} \sin\phi = \left(\frac{\cos\phi}{\Delta H}\right) \frac{1 + y\tan\phi}{1 + y^2} \quad (1a)$$

and its derivative as

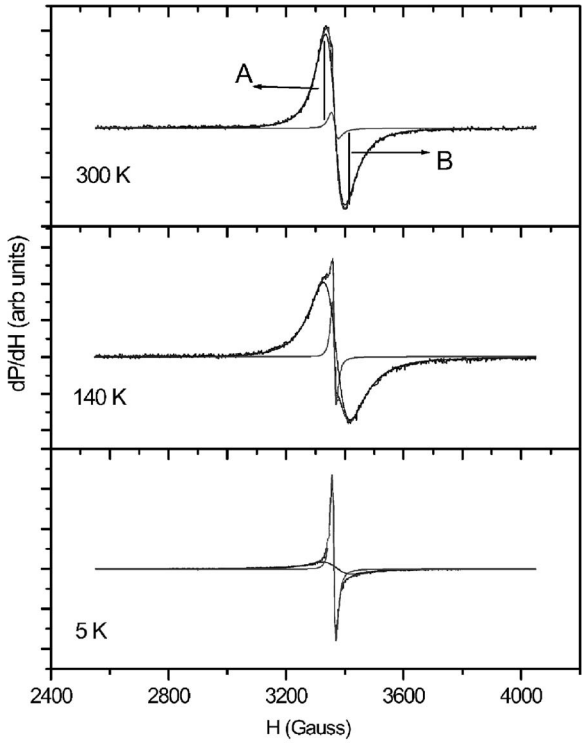

FIG. 2. ESR spectra at 300, 140, and 5 K (shown with the lines separated) for σ=90 S/cm sample.

$$\frac{d\chi}{dH} = \left(\frac{\cos\phi}{\Delta H^2}\right)\frac{-2y + (1-y^2)\tan\phi}{(1+y^2)^2} \tag{1b}$$

or, more simply,

$$\left(\frac{d}{dH}\right)P = \frac{d}{dH}\left(\frac{\Delta H}{\Delta H^2 + (H-H_0)^2} + \frac{\alpha(H-H_0)}{\Delta H^2 + (H-H_0)^2}\right), \tag{2}$$

where χ is the complex susceptibility, $y=(H-H_0)/\Delta H$, ΔH is the linewidth, H_0 the center field, ϕ is the phase shift of the microwave magnetic field in a film sample, resulting from electromagnetic (EM) shielding effect by conducting charge carriers in the sample, and $\alpha=\tan\phi$, the asymmetry parameter is the fraction of the dispersion mixed to the absorption and is directly related to the A/B ratio (for small values of α, $A/B \approx 1+\alpha$). The α value vs temperature is shown in Fig. 3, with the conductivity vs temperature plot in the inset. It is observed that the evolution of α value for the broad line follows the conductivity approximately. The α values show the Dysonian nature of the spectra. The calculated skin depth (at 9.42 GHz) corresponding to σ=90 S/cm is 100 μm, and the thickness of sample is around 30 μm. Therefore, one does not expect a Dysonian to arise when the skin depth is larger than the thickness of the sample, but a weak Dysonian is quite possible.[22] The α values for both narrow and broad lines are nearly the same. One should note that the Dysonian does not necessarily mean that both spin species play equal roles in the screening of the EM field. If any one of the paramagnetic species is supposed to be of free carrier type, which screens out the EM field, then

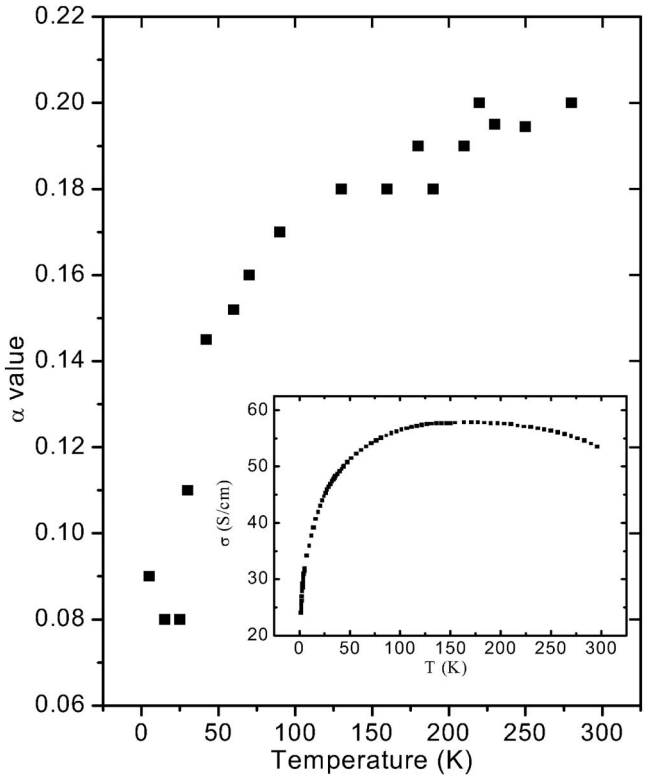

FIG. 3. α value vs temperature for the broad line for σ=90 S/cm sample. The inset shows the temperature dependence of conductivity.

both the lines could show Dysonian line shapes with nearly the same A/B ratio. This screening effect due to any one of conducting species can give raise to asymmetric line shapes in all lines within the range of EM wavelengths.[22] Therefore, the α value should not be taken as a fully characterizing parameter for the motion of the spin species; however, it ensures that at least one of the paramagnetic species has to be of conductive nature. The spectra for 4 and 0.2 S/cm samples ($\alpha \sim 0.1$ for both) are shown in Fig. 4. The nearly equal dominance of both lines for 4 and 0.2 S/cm samples is clear, despite the fact that their conductivity varies by one order of magnitude.

Although the contribution from the narrower signal in 90 S/cm sample is negligible at room temperature, it starts to become dominant as temperature is decreased (see Fig. 2). When the conductivity is lowered from 90 to 10 S/cm by deprotonation, one observes that the ratio of broad line to narrow line areas decreases drastically, yet it remains nearly constant in the conductivity range 4 to 0.2 S/cm (see Fig. 4). In case the narrow line is due to some impurity, then its intensity should have been nearly constant at all doping levels. Furthermore, it was observed that the ratio of lines remains the same at all deprotonation levels, indicating that both spins vary consistently as a function of doping level. This indicates that the narrow fraction is not impervious to deprotonation. Nevertheless, beyond a certain amount of deprotonation, the ratio of the areas is nearly constant, which implies that both the species are created by the doping process. The evolution of the ratio of two lines indicates that the

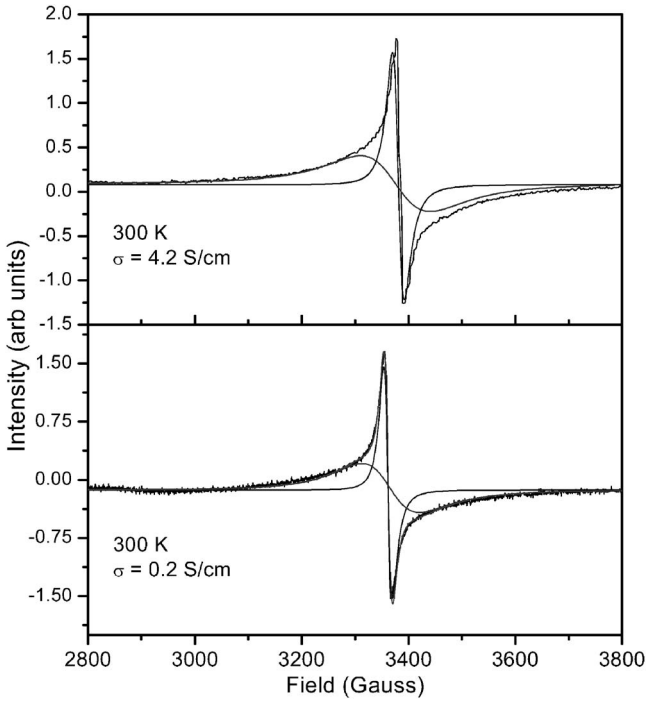

FIG. 4. The spectra at 300 K for conductivities 4 S/cm (top) and 0.2 S/cm (bottom).

spin species responsible for the broad signal get preferentially reduced at mild deprotonation conditions. However, when deprotonation is carried out for a sufficiently long time, both spin species are equally affected. These results suggest that the broad and narrow line spin species are due to delocalized and localized charge carriers in ordered and disordered regions, respectively, in the sample.

The normalized χ (double integrated area under the ESR signal)$\times T$ vs T (300–4 K) is plotted for the two signals (broad and narrow) at values of conductivity (90 and 4 S/cm) in Fig. 5. It is clear that despite the presence of a small Pauli susceptibility in the narrow line for 90 S/cm, the Curie term dominates at lower temperatures. The presence of both Pauli and Curie susceptibility at all temperatures is well known in fully doped conducting polymers like PANI-CSA.[15] The temperature dependence of χT indicates that the Pauli contribution is significantly stronger for the broad line with respect to the narrow line, whereas the Curie contribution is dominant in case of narrow line in 90 S/cm sample. Even in case of 4 S/cm sample the Pauli contribution is significant in the broad line, as in Fig. 5. The large Pauli component in the broad line for 90 S/cm indicates the predominant metallic nature of the spins contributing to the ESR signal.

SQUID measurements were done to confirm the temperature dependence of the ESR susceptibility. The SQUID susceptibility multiplied with temperature, i.e., χT (300–2 K) vs T of the 90 S/cm sample is shown in Fig. 6. Although there is scatter in the data, a rough fit (not shown) to the equation, $\chi T = \chi_P T + C$, where χ_P is Pauli susceptibility and C is Curie's constant, was attempted. The fit estimated a Pauli susceptibility of $\sim 2 \times 10^{-4}$ emu/mol 2-rings and a Curie constant of 3×10^{-2} emu/K/mol 2-rings. The corrections for

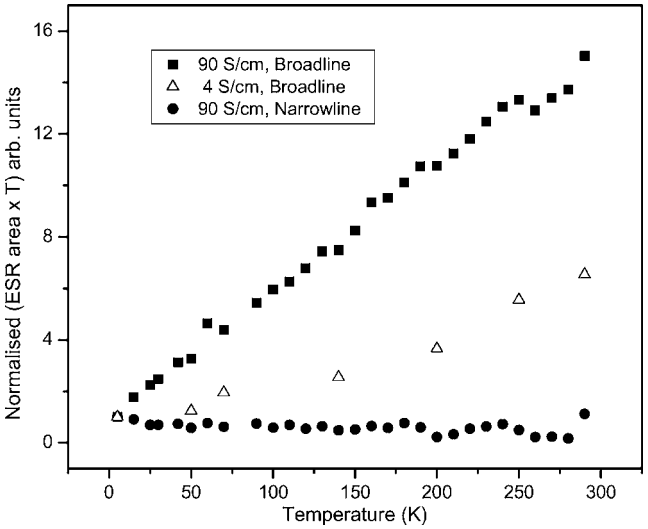

FIG. 5. ESR area$\times T$ ($\propto \chi T$) vs temperature shown for broad and narrow lines, for 90 S/cm and the narrow line for 4 S/cm samples. The areas have been normalized to their respective 5 K values.

the core diamagnetism were done by subtracting the diamagnetism of AMPSA (-8.69×10^{-5} emu/mol) and undoped PANI (-7.85×10^{-5} emu/mol), from the measured values. We assume doping of PANI by AMPSA is 50%, that is, one AMPSA molecule per 2 PANI rings. The Pauli susceptibility corresponds to a density of states (DOS)=3 to 4 states/(eV 2-ring repeat) [or 4/14 =0.3 states/eV/mol(C+N)] and a Curie constant of 2.5 $\times$102 emu/K/mol 2-rings corresponds to roughly 1 spin per 30 rings. Such a larger density, of both types of spins in PANI-AMPSA as compared to PANI-CSA,[15] indicates that the system is optimally doped. The temperature dependence of conductivity of PANI-AMPSA also shows more metallic features than PANI-CSA. Also, a negative magnetoresistance has been observed in PANI-AMPSA, which is not observed in any doped PANI. Therefore a high DOS in PANI-AMPSA is plausible considering these factors. It is significant that

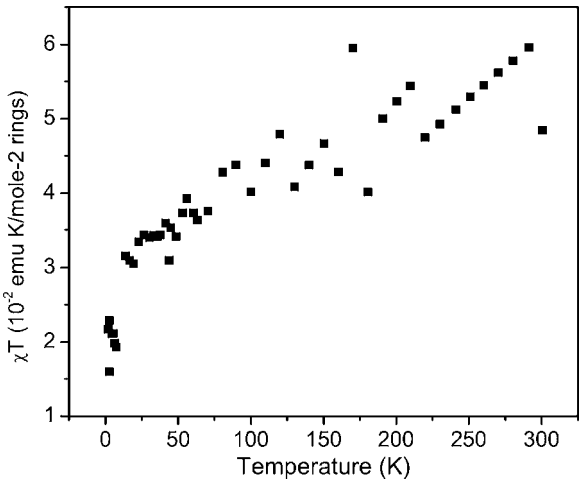

FIG. 6. Susceptibility$\times$temperature of PANI-AMPSA (=90 S/cm) as measured by SQUID.

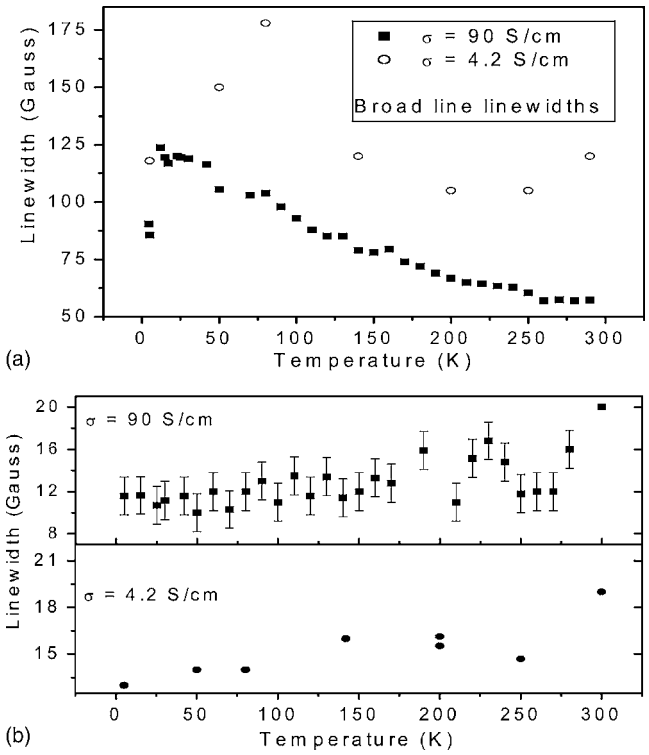

FIG. 7. (a) The linewidth of the broad line vs temperature. Solid square (open circles) indicate data points for 90 S/cm (4 S/cm) samples. (b) The linewidth of the narrow line vs temperature for 90 S/cm (top) and 4 S/cm (bottom) samples.

XRD results for PANI-AMPSA have shown little evidence for crystallinity while PANI-CSA shows crystallinity up to 50%.[17,23]

The susceptibility appears to be the case of Pauli+Curie, indicating that the Pauli and Curie components are present at all temperatures, with the latter becoming stronger at lower temperatures. The Pauli and Curie components are present in both lines, hence both spin species are created by the doping process; in which one of species is trapped in highly disordered or poorly doped regions (relatively not much affected by deprotonation) and gives raise to the narrow line. However, the differences between the temperature dependence of ESR and the SQUID susceptibility data are yet to be investigated in detail with calibrated ESR susceptibility data.

The linewidth vs temperature variations are shown in Figs. 7(a) and 7(b). The broad line shows maxima at 25 and 90 K for 90 and 4 S/cm samples, respectively. The narrow line is nearly temperature independent at all doping levels. In case of broad line for 90 S/cm sample, the linewidth increases from 60 G to a maximum of 120 G, by lowering the temperature from 300 to 25 K; and then it decreases to 85 G at 4 K. This maximum is dependent on the doping level. Such a maximum can occur if the spin species can interact with fixed spin carriers like trapped oxygen or any other paramagnetic spins, via the Houzé-Nechtschein mechanism.[19,20] However, no effect of oxygen on the linewidth was observed. The fixed spin carriers can also be due to any other paramagnetic impurity, but our elemental analyses data from EDAX measurements show that no such impurities are present in the sample. It is also surprising that no oxygen/moisture dependence of linewidth[19] was observed, indicating that the large value of the linewidth is intrinsic to the sample. However, it is known that in some conducting polymers doped with sulfonic acids it is possible to observe such large linewidths, as observed in this work.[24] This suggests that the lone pairs in sulfur can broaden the line, though this is not always observed as in case of CSA doped PANI, as well as other sulphonic acid doped polyanilines.[11]

PANI-CSA and PPy-AMPSA have linewidths of around 2 to 4 G in air, indicating that the role of sulfur in broadening the line is minimal in these cases. In PANI-CSA ($\sim$250 S/cm) the typical value of linewidth is around 0.2 G. However, PANI-AMSPA (2-acrylamido-2-methyl sulphonated *propanoic acid*) has a linewidth of around 25 G, which is relatively large.[24] Moreover, it exhibits a similar temperature dependence of linewidth with a maximum (at $T \sim 25$ K) as in case of PANI-AMPSA system. We believe that the presence of the acryl-amido group [containing both a π-electron group ($CH_2{=}CH$) and a C=O group] indicates a similar origin for the broadening of linewidths. The ability of the C=O bond to make hydrogen bonding with the N—H group is well known, especially when they are in close proximity.[25] The concept of hydrogen bonding has also been invoked to explain self-doping in some systems.[26] Such a hydrogen bonding between the C=O group in AMPSA and the N—H group in PANI chain can bring the chains closer. Furthermore, the π electrons in the $CH_2{=}CH$ group are situated at the end of the AMPSA group, thus the steric hindrance is quite minimal for these π electrons to make a π-π interaction with PANI main chain. These π-π interactions and the hydrogen bonding could enhance the interchain interaction and the self-organization of local molecular scale Q2D structures. This could also explain why PANI-AMPSA does not have any significant oxygen or moisture dependence on the linewidth. According to Kahol *et al.*,[21] the polarons are centered on nitrogen, and the oxygen/water-polaron interaction occurs at this *N* site. This *N* site is not available, due to hydrogen bonding with the amido group, for any significant interaction with oxygen/moisture. This gives a plausible explanation for the anomalies in PANI-AMPSA systems, which are not observed in other sulfonic acid doped PANI samples.

The difference in linewidth between the broad and narrow lines could be ascribed to the difference in the order of PANI chains in various regions in the sample. The more ordered regions have better intermolecular π-electron interaction than the less ordered regions. Especially in case of AMPSA doped PANI, the acrylamido group can enhance the molecular scale ordering of PANI chains via the hydrogen bonding and π-π interaction. This type of intermolecular π-π interactions among various segments in PANI chain can give raise to local Q2D electronic structure in which the charge carriers are fairly delocalized.[27] In fact, the anisotropic sign of transverse (negative) and longitudinal (positive) magnetoresistance in PANI-AMPSA strongly indicates the presence of delocalized carriers in self-assembled Q2D molecular scale structures.[16]

The ESR linewidth can be adequately described by a model developed for quasi-two-dimensional graphite

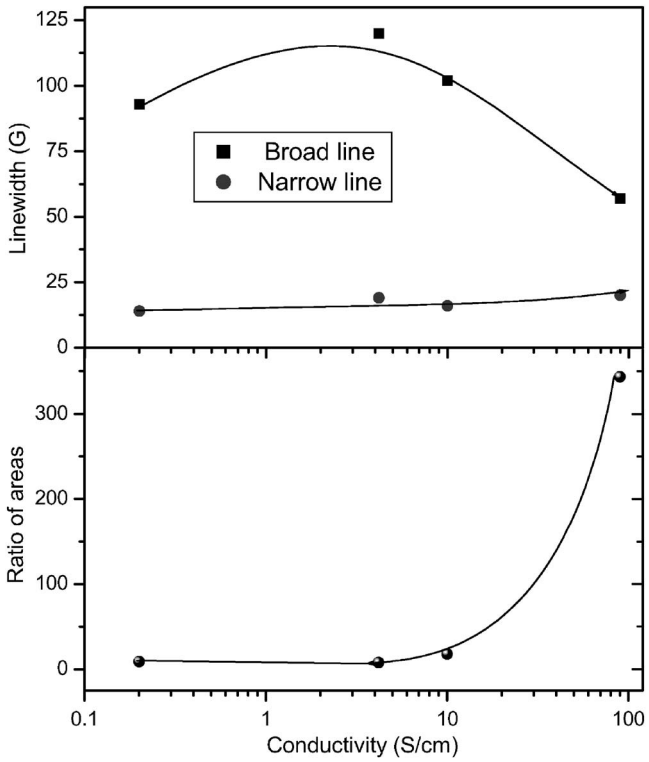

FIG. 8. Linewidths of both lines as a function of conductivity (top). The ratio of broad line area to narrow line area (bottom).

(QTDG) (Refs. 28, 30, and 31). We note that this Q2D structure is similar to that of the basal plane of graphite, although the π-orbital overlap in the case of PANI-AMPSA is expected to be weaker than in graphite, due to the flexible and disordered nature of the polymer chain and the presence of dopants. Based on this observation, a strong exchange interaction can be assumed for this system, where a coupled resonance of itinerant and localized spins can occur, leading to a peak in the linewidth. The temperature dependence of linewidth, in this model, is due to the motional averaging of g values, and the linewidth being dependent upon the motion of the 2D conduction carriers, which in turn is related to the Fermi level and the band structure. It also takes into account of the scattering of charge carriers by both thermal phonons and defects in system. The strongly localized spins, being only around 1% of the total number of spins,[29] do not contribute to transport properties, but play a significant role in the spin relaxation process, especially at low temperatures. Although the temperature dependence of linewidth above $\sim$25 K (90 S/cm) can be explained by the localization of charge carriers, the temperature dependence of conductivity shows a small increase in conductivity till 100 K, showing that the possibility of localization is minimal in that temperature range (i.e., 300–100 K). Moreover the low temperature downturn of linewidth (below 25 K in the 90 S/cm sample and below 100 K in the 4 S/cm sample) cannot be ascribed to delocalization of the charge carriers, when the conductivity shows a fall below 100 K. (See Fig. 8.)

Theoretical calculations based on the band model for Q2D graphite have shown that the "bottleneck effect" in the linewidth can occur at low temperatures, if the interaction with the localized spins is taken into account.[30] The linewidth can be expressed as

$$\Delta H_{pp} = \Delta H_{ie}(\chi_p/\chi_p + \chi_c) + \Delta H_{ls}(\chi_c/\chi_p + \chi_c). \qquad (3)$$

Here, $\Delta H_{pp}(T)$ is the linewidth due to the motional narrowing of g anisotropy, including the contributions from both itinerant electrons (ΔH_{ie}) and localized spins (ΔH_{ls}); χ_p and χ_c are the Pauli and Curie susceptibilities. For a localized defect, the g shift and hence the linewidth should be temperature independent, as has been observed for the narrow line, which is very weakly temperature dependent, as shown in Fig. 7(b).

We note that according to the Q2D model developed for graphene sheet, the linewidth due to the localized spins is estimated to be around 10 G, with weak or hardly any temperature dependence.[30] Hence it is expected that the linewidth of the ESR line due to localized carriers in PANI-AMPSA would be around 10 G, and the measured value of 11 G, for the narrow line, is quite agreeable with the above estimate. Moreover, it is nearly temperature independent, consistent with the theoretical description for a localized spin in this model.

In the above graphene sheet model the surface states can contribute significantly to the linewidth.[31] In the extended model by taking into account the surface states, a thickness dependence of the linewidth has been predicted. This contribution of the surface states is related to the difference in the average probability of spin flipping due to scattering of charge carriers at the surface. This model states

$$\Delta H_{ie} = \Delta H_{ie}^{\text{surf}} + \Delta H_{ie}^{\text{intr}}, \qquad (4)$$

where $\Delta H_{ie}^{\text{surf}}$ is the contribution from sample surface to the spin relaxation and $\Delta H_{ie}^{\text{intr}}$ is the contribution from defects buried inside the sample. Hence we have carried out a thickness dependence of linewidth. A similar dependence of linewidth on the thickness of the sample (PANI-AMPSA) was observed. At $\sim$20 (35) micron the linewidth of the broad line is 186 G (60 G), at room temperature, consistent with this framework.

A comparison between the temperature dependence of linewidths of the ESR lines of PANI-AMPSA (90 S/cm) broad line, multiwall carbon nanotubes (MWNT), highly oriented pyrolitic graphite (HOPG) is shown in Fig. 9. All of them exhibit a low temperature peak in the linewidth. The linewidth increases till a certain temperature, and then it decreases. The rather broad peak of MWNT is at 100 K, presumably because of the warped nature of the graphene sheets. It is observed that the linewidth dependence of PANI-AMPSA broad line is closer to that of graphite, with a similar low temperature peak at $\sim$20 K. However, exact calculations for linewidth/spin relaxation due to various spin species are yet to be determined from the precise theoretical values for the parameters in Eq. (4). However this qualitative level description shows the applicability of the Q2D model for explaining the ESR signals and spin relaxation in the case of PANI-AMPSA.

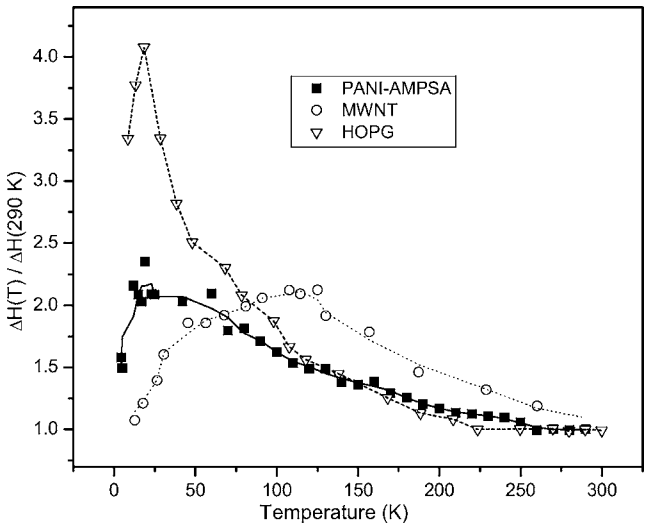

FIG. 9. The temperature dependence of linewidths for PANI-AMPSA, MNWT, and HOPG. The linewidths have been normalized to their respective room temperature (290 K) values, i.e., 57.3 G for PANI-AMPSA, 15.1 G for MWNT, and 4.8 G for HOPG (basal plane).

IV. CONCLUSION

The X-band ESR spectra of PANI-AMPSA indicate the presence of two types of spin carriers. Taking into account of the temperature and doping dependence of linewidths, we suggest that the broad and narrow lines are contributions from the delocalized and localized charge carriers, respectively. The temperature behavior of both the lines are explained in terms of the Q2D model, where a strong interaction is presumed to arise between the itinerant and localized spins, leading to a peak in the of linewidth at low temperatures. There is also a contribution to the linewidth from the surface states as observed from the thickness dependence of linewidth. A resemblance of the temperature dependence of linewidth of PANI-AMPSA to that of graphite is noted. A strong Pauli susceptibility of the spin species is associated with the broad line is observed, and this indicates that the sample is intrinsically metallic in Q2D regions in PANI-AMPSA sample.

ACKNOWLEDGMENT

We thank Janhavi Joshi for help with the experiments.

[1] K. Mizoguchi, Synth. Met. **119**, 35 (2001).
[2] M. Nechtschein, in *Handbook of Conducting Polymers*, 2nd ed., edited T. A. Skotheim, R. Elsenbaumer, and J. R. Reynolds (Marcel Dekker Inc., New York, 1998), p. 141.
[3] Z. H. Wang, C. Li, E. M. Scherr, A. G. MacDiarmid, and A. J. Epstein, Phys. Rev. Lett. **66**, 13 (1991); **66**, 1745 (1991).
[4] Z. H. Wang, E. M. Scherr, A. G. MacDiarmid, and A. J. Epstein, Phys. Rev. B **45**, 4190 (1992).
[5] J. P. Travers, P. Le Guyadec, P. N. Adams, P. J. Laughlin, and A. P. Monkman, Synth. Met. **65**, 159 (1994).
[6] K. Mizoguchi and S. Kuroda, in *Handbook of Organic Conducting Molecules and Polymers, Vol. 3*, edited by H. S. Nalwa (John Wiley and Sons, Ltd., New York, 1997), p. 251.
[7] K. Mizoguchi, M. Nechtschein, J.-P. Travers, and C. Menardo, Phys. Rev. Lett. **63**, 66 (1989).
[8] A. G. Macdiarmid, J. C. Chiang, A. F. Richter, and A. J. Epstein, Synth. Met. **18**, 285 (1987).
[9] R. Menon, C. O. Yoon, D. Moses, A. J. Heeger, and Y. Cao, Phys. Rev. B **48**, 17685 (1993).
[10] M. Reghu, Y. Cao, D. Moses, and A. J. Heeger, Phys. Rev. B **47**, 1758 (1993).
[11] P. K. Kahol, K. K. Satheesh Kumar, S. Geetha, and D. C. Trivedi, Synth. Met. **139**, 191 (2003).
[12] *Handbook of Conducting Polymers*, edited by T. A. Skotheim (Dekker, New York, 1986).
[13] A. J. Heeger, S. Kivelson, J. R. Schrieffer, and W. P. Su, Rev. Mod. Phys. **60**, 781 (1988).
[14] F. Genoud, J. Kruszka, M. Nechtschein, C. Santier, S. Davied, and Y. Nicolau, Synth. Met. **41–43**, 2887 (1991).
[15] N. S. Sariciftci, A. J. Heeger, and Y. Cao, Phys. Rev. B **49**, 5988 (1994).
[16] A. K. Mukherjee and R. Menon, Synth. Met. **119**, 427 (2001); A. K. Mukherjee and R. Menon, J. Phys.: Condens. Matter **17**, 1 (2005).
[17] G. Tzamalis, N. A. Zaidi, C. C. Homes, and A. P. Monkman, Phys. Rev. B **66**, 085202 (2002).
[18] P. N. Adams, P. Devasagayam, S. J. Pomfret, L. Abell, and A. P. Monkman, J. Phys.: Condens. Matter **10**, 8293 (1998).
[19] E. Houze and M. Nechtschein, Phys. Rev. B **53**, 14309 (1996).
[20] K. Mizoguchi, N. Kata, H. Sakamoto, K. Yoshioka, S. Masubuchi, and S. Kazama, Solid State Commun. **105**, 81 (1998).
[21] P. K. Kahol, A. J. Dyakonov, and B. J. McCormick, Synth. Met. **89**, 17 (1997).
[22] H. Kodera, J. Phys. Soc. Jpn. **28**, 89 (1970).
[23] G. Tzamalis, N. A. Zaidi, C. C. Homes, and A. P. Monkman, J. Phys.: Condens. Matter **13**, 6297 (2001).
[24] W. P. Lee, K. R. Brenneman, A. D. Gudmundsdottir, M. S. Platz, P. K. Kahol, A. P. Monkman, and A. J. Epstein, Synth. Met. **101**, 819 (1999).
[25] N. Kuhnert and A. Le-Gresley, Chem. Commun. (Cambridge) **2003**, 2426 (2003) and references therein.
[26] K. R. Brenneman, J. Feng, Y. Zhou, A. G. MacDiarmid, P. K. Kahol, and A. J. Epstein, Synth. Met. **101**, 785 (1999).
[27] M. Wohlgennant, X. M. Jiang, and Z. V. Vardeny, Phys. Rev. B **69**, 241204(R) (2004).
[28] A. S. Kotosonov and D. V. Shilo, Carbon **36**, 1649 (1998).
[29] We approximately take the ratio of the localized carriers to the conduction electrons, in the ordered regions, from the measured ratio of the area of the narrow line to the broad line (=1 : 343, that is less than 1%), as from Fig. 8.
[30] V. Likodimos, S. Glenis, N. Guskos, and C. L. Lin, Phys. Rev. B **68**, 045417 (2003).
[31] A. M. Ziatdinov and V. V. Kainara, in *EPR in the 21st Century*, edited by A. Kawamori, J. Yamauchi, and H. Ohta (Elsevier Science B. V. Amsterdam, 2002), pp. 293–297.